Probabilistically assessing the role of nutrient loading in harmful algal bloom formation in western Lake Erie

Isabella Bertani [a,*], Daniel R. Obenour [b], Cara E. Steger [a,1], Craig A. Stow [c], Andrew D. Gronewold [c], Donald Scavia [a]

[a] Water Center, Graham Sustainability Institute, University of Michigan, 625 E. Liberty St., Suite 300, Ann Arbor, MI 48104, USA
[b] Department of Civil, Construction, and Environmental Engineering, North Carolina State University, Campus Box 7908, Raleigh, NC27695-7908, USA
[c] NOAA Great Lakes Environmental Research Laboratory, 4840 S. State Rd., Ann Arbor, MI 48108, USA

ARTICLE INFO

ABSTRACT

Harmful algal blooms (HABs) have increased in frequency and magnitude in western Lake Erie and spring phosphorus (P) load was shown to be a key driver of bloom intensity. A recently developed Bayesian hierarchical model that predicts peak bloom size as a function of Maumee River phosphorus load suggested an apparent increased susceptibility of the lake to HABs. We applied that model to develop load–response curves to inform revision of Lake Erie phosphorus load targets under the 2012 Great Lakes Water Quality Agreement. In this application, the model was modified to estimate the fraction of the particulate P (PP) load that becomes bioavailable, and it was recalibrated with additional bloom observations. Although the uncertainty surrounding the estimate of the bioavailable PP fraction is large, inclusion in the model improves prediction of bloom variability compared to dissolved reactive P (DRP) alone. The ability to characterize model and measurement uncertainty through hierarchical modeling allowed us to show that inconsistencies in bloom measurement represent a considerable portion of the overall uncertainty associated with load–response curves. The updated calibration also lends support to the system's apparent enhanced susceptibility to blooms. The temporal trend estimated by the model results in an upward shift of the load–response curve over time such that a larger load reduction is required to achieve a target bloom size today compared to earlier years. More research is needed to further test the hypothesis of a shift in the lake's response to stressors over time and, if confirmed, to explore underlying mechanisms.

Introduction

The implementation of primarily point-source phosphorus (P) reduction programs under the 1978 Great Lakes Water Quality Agreement (GLWQA) was followed by a decrease in the occurrence of algal blooms and hypoxia in Lake Erie during the 1980s (DePinto etal., 1986; Makarewicz etal., 1989). However, harmful algal blooms (HABs) have increased in frequency and intensity since the mid-1990s in the lake's western basin (Bridgeman etal., 2013; Scavia etal., 2014; Stumpf etal., 2012), and especially large blooms have been recorded in recent years. The 2011 bloom was the largest on record since systematic HAB monitoring began in 2002 (Michalak etal., 2013), and a preliminary satellite image analysis suggests that the 2015 bloom surpassed that of 2011 (http://tinyurl.com/lxqnyro, accessed on 30 November 2015; Schaeffer etal., 2015). These cyanobacteria blooms, which are generally dominated by *Microcystis* spp. (Bridgeman etal., 2012; Brittain etal., 2000; Chaffin etal.,

2013), have been compromising the safety of beaches and drinking water supplies, culminating with a 3-day "do not drink" advisory issued by the City of Toledo in the summer of 2014 that affected over 400,000 people (Cha and Stow, 2015; Jetoo etal., 2015). Several studies identified phosphorus load from the Maumee River as a key driver of western Lake Erie bloom intensity (Michalak etal., 2013; Obenour etal., 2014; Stumpf etal., 2012), although other biophysical factors likely contribute to interannual variability, such as climate-induced shifts in the timing, frequency, and intensity of extreme weather events (Michalak etal., 2013; Steffen etal., 2014), impact of invasive species (Conroy etal., 2005; Vanderploeg etal., 2001), and late-summer nitrogen co-limitation (Chaffin etal., 2013).

Toxic and nuisance algal blooms are among the key eutrophication-related issues identified in the Great Lakes Water Quality Agreement Amendment of 2012 Nutrient Annex (GLWQA, 2012) that calls for a review and update of the 1978 phosphorus load targets. Estimating the nutrient load reductions necessary to achieve target bloom sizes requires models capable of quantifying the relationship between load and bloom severity. Accurate quantification of the uncertainty associated with the load–bloom relationship is also critical to provide policy makers with defensible ranges of likely future bloom sizes corresponding to different P load scenarios. Quantified uncertainty should be

* Corresponding author. Tel.:+1 734 763 0688; fax:+1 734 647 6730.
  E-mail address: ibertani@umich.edu (I. Bertani).
[1] Present address: Graduate Degree Program in Ecology, Natural Resource Ecology Lab, Colorado State University, Campus Delivery A245, Fort Collins, CO80523-1499, USA.

recognized as essential information in the decision process (Reckhow, 1994; Reckhow and Chapra, 1999) and is particularly important when modeling a phenomenon like cyanobacteria blooms, where substantial limitations and uncertainties are known to affect the methods used to measure bloom size (Ho and Michalak, 2015; Reinart and Kutser, 2006; Srivastava etal., 2013), as well as our knowledge of the multiple interacting processes that influence bloom formation (Perovich etal., 2008). Failure to account for these sources of variance could lead to models that do not accurately reflect our actual knowledge of the system's behavior.

Obenour etal. (2014) developed a probabilistic model that relates spring phosphorus load from the Maumee River to peak summer HAB size in western Lake Erie. Through adoption of a Bayesian hierarchical approach, the model accounts for multiple sources of uncertainty and separates process error from measurement error. The original model calibration, based on two distinct sets of annual bloom size estimates measured in 2002–2013, identified spring (February–June) total phosphorus (TP) load from the Maumee River as the best performing bloom predictor (Obenour etal., 2014). A positive temporal trend was also revealed within the model, suggesting an apparent gradual increase in the lake's susceptibility to large blooms over the years (Obenour etal., 2014). Notably, the use of nitrate or dissolved reactive phosphorus (DRP) loads as alternative bloom predictors resulted in lower predictability, while the temporal trend remained significantly positive (Obenour etal., 2014). These results suggest that the increase in the DRP portion of the Maumee TP load observed since the 1990s (Baker etal., 2014a; Stow etal., 2015) may not be sufficient to explain the apparent enhanced vulnerability of western Lake Erie to HAB formation. DRP is generally considered to be readily available for algal uptake, as confirmed by bioassay studies conducted in the Maumee River (Lambert, 2012), thus representing an immediate source of P to fuel algal growth. The other main portion of the TP load– the particulate phosphorus (PP) load (Baker etal., 2014a) – was found to be only partially available to algae by several studies conducted on samples taken in the Maumee River (Table1). However, less is known about the ultimate bioavailability of the spring Maumee PP load after it enters the western basin and undergoes in-lake physical, chemical, and biological transformations, including adsorption/desorption, dissolution/precipitation, and diffusion of phosphate from sediment particles, recycling by lake biota, and decomposition and mineralization of organic P compounds (Andersson etal., 1988; Boström etal., 1988a; Carpenter etal., 1992; Søndergaard etal., 2003). Although PP settles quickly (Baker etal., 2014b), sediment re-suspension occurs frequently in western Lake Erie (Boegman etal., 2008; Guildford etal., 2005). However, the role of sediment phosphorus re-suspension in promoting

algal production is still poorly understood. Furthermore, dreissenid mussels, which were first observed in the lake in 1986 (Carlton, 2008), have the potential to enhance in-lake PP recycling as DRP (Arnott and Vanni, 1996; Conroy etal., 2005; Mellina etal., 1995). In view of these considerations, the GLWQA Nutrient Annex analysis required models to account for the bioavailable fraction of the P load when generating load–response curves (GLWQA, 2012).

Here, we apply the model developed by Obenour etal. (2014) to produce load–response curves as part of a multi-model approach that informed revision of the GLWQA P load targets for Lake Erie (Scavia etal., 2016-in this issue; GLWQA, 2015). In this work, we modify the original model to allow for the differentiation between DRP and PP loads and for the empirical estimation of the fraction of the PP load that becomes bioavailable over the summer and contributes to bloom development. The model is also recalibrated to updated and expanded sets of bloom observations, including new bloom estimates for the years 2013 and 2014. The updated model calibration is compared to the original calibration (Obenour etal., 2014), to assess the effects of adding the most recent bloom observations on the positive trend in HAB susceptibility originally estimated by the model.

Methods

Bayesian HAB model

The probabilistic forecasting model developed by Obenour etal. (2014) predicts peak late-summer bloom size in western Lake Erie given spring nutrient load from the Maumee River, and a temporal trend. The temporal trend reflects the lake's apparent increasing susceptibility to HABs, such that smaller P loads initiate larger blooms at the end of the study period than at the beginning. The model is solved within a Bayesian hierarchical framework that allows for simultaneous calibration to multiple sets of bloom observations and for a differentiation between model prediction (i.e., process) error and bloom measurement error (Obenour etal., 2014). The model functions in "scenario mode" (this application) as well as in "forecasting mode", and it has recently been incorporated into an ensemble approach developed by the National Oceanic and Atmospheric Administration to provide seasonal forecasts of peak summer HAB severity (http://tinyurl.com/og62lbh, accessed on 30 November 2015).

Three candidate models using different probability distributions (normal, lognormal, and gamma) to characterize error terms were compared (Obenour etal., 2014), and in this application, we use the "gamma model", which was found to perform best. Particularly, the model explained over 80% of the year-to-year variability in peak bloom size over the study period of 2002–2013 (as determined through model cross validation) (Obenour etal., 2014). The deterministic component of the model is as follows:

$$\hat{z}_i = \begin{cases} \beta_b + \beta_0 + \beta_w W_i + \beta_t T_i & \text{for } \beta_0 + \beta_w W_i + \beta_t T_i > 0 \\ \beta_b & \text{for } \beta_0 + \beta_w W_i + \beta_t T_i < 0 \end{cases} \quad (1)$$

where $\beta_b, \beta_0, \beta_w,$ and β_t are model parameters that predict bloom size, $\hat{z}_i$, in year i, in terms of spring nutrient load, W_i, and model year, T_i. The parameter β_b is a background bloom level representing bloom size in years of small nutrient load. As load increases beyond a critical threshold, the size of the bloom increases as a linear function of the load, and the parameter β_w represents the unit increase in bloom size per unit increase in load. The parameter β_0 is an intercept term, and $\beta_t T_i$ essentially allows the intercept to change over time. The lake's apparent increasing susceptibility to HABs is reflected by a positive value of β_t such that the intercept increases gradually over time (Obenour etal., 2014). The intercept is inversely related to the load threshold required to increase bloom size beyond the background level. Model predictions are related to bloom

Table1
Literature on Maumee River PP bioavailability reviewed to develop the loosely informative prior for the parameter θ. The Method column indicates whether the bioavailable fraction of PP was estimated indirectly through NaOH extraction or directly through algal bioassays. Reported values are generally averages of multiple samples. Whenever a measure of uncertainty was available in the original study (r: range of measured values; c.v.: coefficient of variation; s.d.: standard deviation), we reported it.

Year	Method	Bioavailable PP fraction	Reference
1977	NaOH	41.9%	Logan etal. (1979)
1977–1978	NaOH	34% (c.v. 14%)	Armstrong etal. (1979)
1980	R-NaOH	20.3% (r: 18.5%–23.6%)	DePinto etal. (1981)
1980	NaOH	30.1% (r: 26.0%–41.2%)	DePinto etal. (1981)
1980	Bioassay	25.3% (r: 15.6%–37.9%)	DePinto etal. (1981)
1981	R-NaOH	24%	Young etal. (1985)
1981	NaOH	37%	Young etal. (1985)
1981	Bioassay	26%	Young etal. (1985)
2010	NaOH	41% ± 1% s.d.	Lambert (2012)
2010	Bioassay	37% ± 2% s.d.	Lambert (2012)
1982	NaOH	28%	Baker etal. (2014a)
2007–2008	NaOH	26.2%	Baker etal. (2014a)
2009–2010	NaOH	20.1%	Baker etal. (2014a)

observations, $z_{i,j}$, through the following probabilistic expressions:

$$z_{i,j} \sim \text{Gamma}\left[(\hat{z}_i + \gamma_i)^2/\sigma_\epsilon^2, \quad (\hat{z}_i + \gamma_i)/\sigma_\epsilon^2\right] \quad (2)$$

$$\gamma_i \sim \text{Gamma}\left(\hat{z}_i^2/\sigma_\gamma^2, \hat{z}_i/\sigma_\gamma^2\right) - \hat{z}_i \quad (3)$$

Model prediction errors (γ_i) are drawn from a gamma distribution with variance σ_γ^2, and observation measurement errors are drawn from a gamma distribution with variance σ_ϵ^2. Subscript j differentiates between two distinct sets of observations of annual bloom size (see next section).

For each year i, the spring nutrient load is determined as a weighted average of January to June ($m = 1$ to 6) monthly loads $w_{i,m}$, based on the following equations:

$$W_i = \frac{1}{\sum \psi_m} \sum_{m=1}^{6} w_{i,m} \psi_m \quad (4)$$

$$\psi_m = \begin{cases} 0 & \text{for } m \le \left(\beta_\psi - 1\right) \\ m + 1 - \beta_\psi & \text{for } \left(\beta_\psi - 1\right) < m < \beta_\psi \\ 1 & \text{for } m \ge \beta_\psi \end{cases} \quad (5)$$

where β_ψ is a weighting parameter estimated probabilistically within the model. A more detailed description of the model formulation can be found in Obenour etal. (2014).

Updated calibration dataset

The original model was calibrated to two sets of annual bloom size estimates, one derived from satellite imagery (2002–2012) (Stumpf etal., 2012) and the other from in situ plankton sampling (2002–2013) (Bridgeman etal., 2013). As in the original model application, the 2011 satellite bloom estimate used in this study is lower than what reported in Stumpf etal. (2012) because we excluded dates when the bloom moved far into the central basin (October 2011) to ensure consistency with other years, when the bloom was generally confined to the western basin (Obenour etal., 2014). Since the original model publication, bloom estimates for more recent years have become available both for the "Stumpf" remote sensing dataset (2013–2014) (R. Stumpf, personal communication, 2015) and for the "Bridgeman" in situ data set (2014) (T. Bridgeman, personal communication, 2015). Furthermore, the 2013 insitu bloom estimate has been revised (T.Bridgeman, personal communication, 2015). For this application, we recalibrated the model to the revised and expanded sets of bloom estimates, which are generally consistent in showing an overall increase in bloom size over the study period (Fig.1a).

Bioavailable phosphorus load as nutrient predictor

The original model was calibrated using the spring Maumee TP, DRP, or nitrate loads as alternative candidate nutrient predictors, and TP was found to be the best predictor (Obenour etal., 2014). In this study, we focus our analyses on P (rather than nitrogen), which is the target nutrient considered within the GLWQA Nutrient Annex effort (GLWQA, 2012). For this application, the original model formulation has been modified to develop an estimate of bioavailable Maumee P load. Specifically, the bioavailable P load was estimated as the sum of the bioavailable portions of the DRP and PP loads (Baker etal., 2014a; Lee etal., 1980):

$$W_i = \text{Bioavailable } P_i = \eta \text{DRP}_i + \theta \text{PP}_i \quad (6)$$

The PP load was calculated as the difference between the TP and DRP loads (Baker etal., 2014a). Based on a review of the literature on the
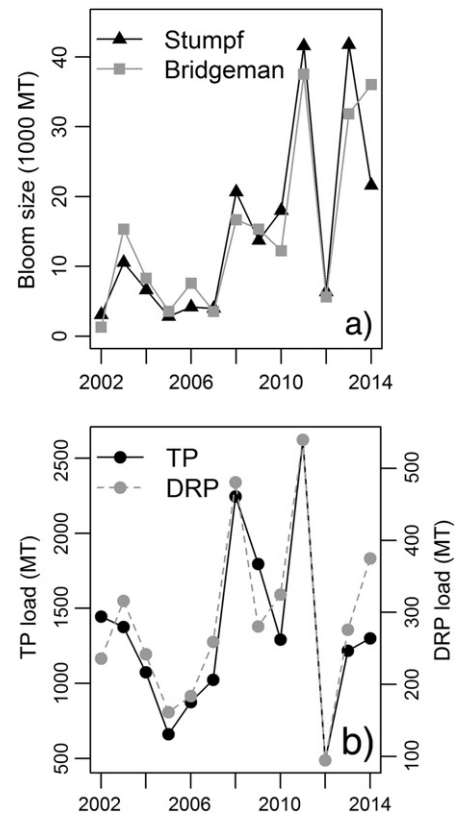

Fig.1. (a) Peak summer bloom size in western Lake Erie over the period 2002–2014 according to remote sensing (Stumpf) and in situ sampling (Bridgeman) estimates. (b)Spring (February–June) cumulative TP and DRP loads delivered to western Lake Erie by the Maumee River over the period 2002–2014. For details on data sources and estimation methods see the "Methods" section. MT indicates metric tons.

bioavailability of different P forms in the Maumee River, DRP is expected to be approximately 100% readily available to algae ($\eta = 1$) (Lambert, 2012), while only a fraction (θ) of the PP load is expected to become available to algae (Table1). The parameter θ was thus estimated probabilistically, together with other model parameters, through Bayesian inference. For brevity, we refer to this revised model formulation as the "bioavailable P model", as opposed to the "TP model" and "DRP model", which use TP and DRP loads as the bloom predictor, respectively. To compare results of the model calibration based on bioavailable P load to those obtained using TP and DRP loads, we also recalibrated both the TP and DRP models to the updated 2002–2014 bloom observations (Electronic Supplementary Material (ESM) TableS4). TP and DRP loads for the period 2002–2014 (Fig.1b) were calculated from Maumee River nutrient concentration data measured by Heidelberg University's National Center for Water Quality Research (NCWQR, http://www.heidelberg.edu/academiclife/distinctive/ncwqr/data, accessed on 2 September 2015), and stream flow data measured by the United States Geological Survey (USGS, http://www.usgs.gov/water, accessed on 2 September 2015) using the same methods outlined in Obenour etal. (2014).

Model calibration

The model was calibrated to the two sets of bloom observations through Bayesian inference using a Markov Chain Monte Carlo (MCMC) sampling algorithm implemented within the WinBUGs software, interfaced with R through the R package R2WinBUGS (Lunn etal., 2000; R Core Team, 2015; Sturtz etal., 2005). Detailed information on the MCMC algorithm settings, chain convergence evaluation, and parameter prior distributions can be found in Obenour etal. (2014). To develop a loosely informative prior for θ, we reviewed the bioavailable PP

fractions reported in P fractionation analyses and algal bioavailability assays conducted in the Maumee River (Table1). While algal bioassays are the preferable method to directly estimate the biological availability of sediment-bound P (Lee etal., 1980), the fraction of PP that is obtained through NaOH extraction was found to correlate closely with results from algal bioassays (DePinto etal., 1981; International Joint Commission, 1980) and is often used as a proxy for the overall amount of inorganic PP likely to become available to algae (Armstrong etal., 1979; Baker etal., 2014a). We used a vague normal prior distribution (mean = 0.3 and standard deviation = 0.7) that is constrained to be between 0.2 and 1, resulting in a mode of 0.3 and an effective mean of 0.57. The normal distribution was given a mean of 0.3 because the bioavailable fraction of PP in the Maumee was generally reported to be between 0.2 and 0.4 (Table1). The lower limit (0.2) reflects the fact that at least 20% of the Maumee River PP is expected to be readily bioavailable (Table1). The upper limit (1) allows the model to potentially estimate values for θ larger than the maximum values measured in the Maumee River (Table1) to account for potential in-lake biogeochemical processes that may cause more PP to become available throughout the summer (Boström etal., 1988b; Lee etal., 1980). To assess the model's performance when predicting data not included in the calibration process, a leave-one-year-out cross validation was carried out where observations from each year were removed from the data set one at a time in turn, and the recalibrated model was used to predict the excluded observations (Obenour etal., 2014).

Load–response curve development

As part of the GLWQA Nutrient Annex modeling effort, the model was used to generate load–response curves estimating the expected range of bloom sizes corresponding to different P load reduction scenarios. The following scenarios were implemented:

1. We varied the TP load (PP and DRP) between 20 and 554 MT/mo, roughly corresponding to 5%–150% of the 2008 weighted TP load (376 MT/mo) (Fig. 3 and ESM TableS1).
2. We varied the PP load between 16 and 437 MT/mo, roughly corresponding to 5%–150% of the 2008 weighted PP load (297 MT/mo), while holding the DRP load constant at 2008 levels (Fig. 4a and ESM TableS2).
3. We varied the DRP load between 4 and 117 MT/mo, roughly corresponding to 5%–150% of the 2008 weighted DRP load (79 MT/mo), while holding PP constant at 2008 levels (Fig. 4b and ESM TableS3).

Because the model includes a temporal trend component, reflecting the system's apparent increasing susceptibility to algal blooms, we developed response curves for both 2008 (year chosen as baseline scenario within the Nutrient Annex effort) and 2014 (approximately current) lake conditions.

Results

Updated model calibration

The TP and DRP models, recalibrated to the 2002–2014 bloom observations (TableS4), explained less of the inter-annual HAB variability (TP model: R^2 = 84.9%; DRP model: R^2 = 77.4%) compared to the original calibration data set (TP model: R^2 = 91.9%; DRP model: R^2 = 88.0%; Obenour etal., 2014). The bioavailable P model performed similarly to the TP model (R^2 = 84.2%), with the largest discrepancies between observed and predicted bloom sizes occurring for the 2013–2014 Stumpf estimates (Fig.2a). A similar decrease in model skill was observed when performing a leave-one-year-out cross validation, with the TP and bioavailable P models calibrated to the new observations resulting in a cross validation (CV) R^2 of 73.7% and 69.8% (Fig.2b), respectively, compared to a CV-R^2 = 83.8% for the original TP model (Obenour etal., 2014).
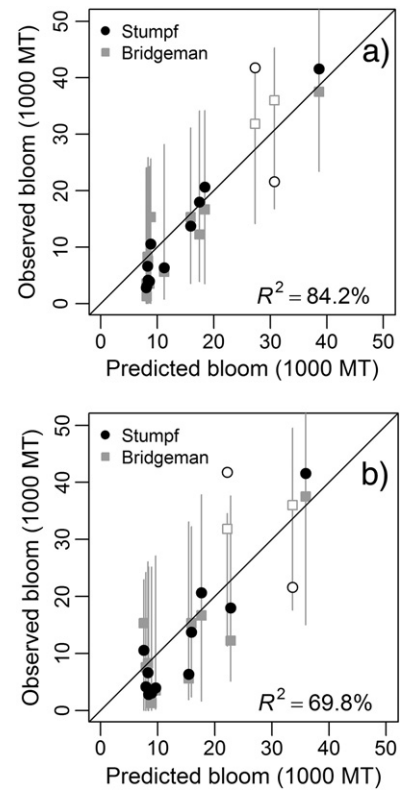

Fig.2. Bioavailable P model calibrated to the bloom estimates shown in Fig.1: observed versus predicted bloom sizes with 95% predictive intervals accounting for model prediction error, bloom measurement error, and parameter uncertainty. (a) Full model performance; (b) cross validation model performance. The 2013 and 2014 observations are indicated by empty symbols.

Posterior parameter mean estimates and their 95% credible intervals (Table 2 and ESM TableS4) were similar for the models using either TP or bioavailable P, with the exception of the parameter β_w. β_w quantifies the rate of change in bloom size per unit of load, and the larger value estimated by the bioavailable P model reflects the fact that the latter represents only a fraction of the overall TP load. Compared to the original TP model calibration, the updated model resulted in an increased estimated mean value for the temporal trend parameter β_t, from 2680MT/year to 3700 and 3570 MT/year for the updated TP and bioavailable P models, respectively (Table 2 and ESM TableS4). The updated DRP model also showed a positive temporal trend (2950 MT/year), although the mean estimated value did not change from the original calibration (2940 MT/year; D. Obenour, personal communication, 2015). A marked increase was also observed in the mean estimated value of σ_ϵ, representing the standard deviation associated with bloom measurement error (from 2690 MT for the original calibration data set to approximately 5100 MT for the updated models; Table 2 and ESM TableS4). The standard

Table2
Posterior parameter means and 95% credible intervals estimated by the bioavailable P model calibrated to the bloom estimates shown in Fig.1. A detailed description of model parameters and prior distributions can be found in Obenour etal. (2014).

Parameter	Units of measurement	Mean	95% CI
β_0	1000 MT	−18.9	−37.0 – −0.6
β_w	1000 MT/(1000 MT/month)	111.8	51.6 – 191.3
β_b	1000 MT	7.91	4.34 – 11.86
β_t	1000 MT/year	3.57	1.32 – 5.95
β_ψ		2.46	1.09 – 4.29
σ_ϵ	1000 MT	5.07	3.18 – 7.47
σ_γ	1000 MT	3.14	0.18 – 7.14
θ		0.63	0.25 – 0.98

deviation associated with model prediction error, σ_γ, showed less of an increase, from 2630 MT for the original TP model to 2880 MT and 3140 MT for the updated TP and bioavailable P model, respectively (Table 2 and ESM TableS4). The average bioavailable fraction of the PP load (θ) estimated by the model is 63%, although the uncertainty surrounding this estimate is large, indicating that the existing model and data have limited ability to resolve this parameter (Table2).

Load–response scenarios

The ability of the model to separate measurement error from model prediction error allowed us to illustrate the contribution of each source of variance to the overall uncertainty associated with the load–response curves (Figs.3 and 4). However, only model prediction error is of interest when developing load–response curves to inform management plans. Hence, the 95% predictive intervals associated with the model predictions provided for this purpose (ESM TablesS1, S2, and S3) are based on model prediction and parameter uncertainty only (dashed lines in Figs.3 and 4) and do not account for bloom measurement error (dotted lines in Figs.3 and 4).

Separating the TP load into DRP and PP within the bioavailable P model allowed us to explore the likely ranges of bloom sizes associated with load reduction scenarios that could potentially be designed to address different components of the overall TP load (Figs.3 and 4 and ESM TablesS1, S2, and S3). Within this modeling effort, cyanobacteria blooms in western Lake Erie are classified as "severe" when they reach an overall biomass >9600 MT (Scavia etal., 2016-in this issue). The updated cyanobacteria model predicts that under 2008 lake conditions (gray lines in Figs.3 and 4), a spring Maumee TP load below 230 MT/month would be necessary to keep peak summer bloom size below 9600 MT (95% predictive interval: 2500–20,000 MT) (Fig.3 and ESM TableS1). If only the PP fraction of the TP load is reduced, while holding DRP constant at 2008 levels, the model estimates that a spring PP load
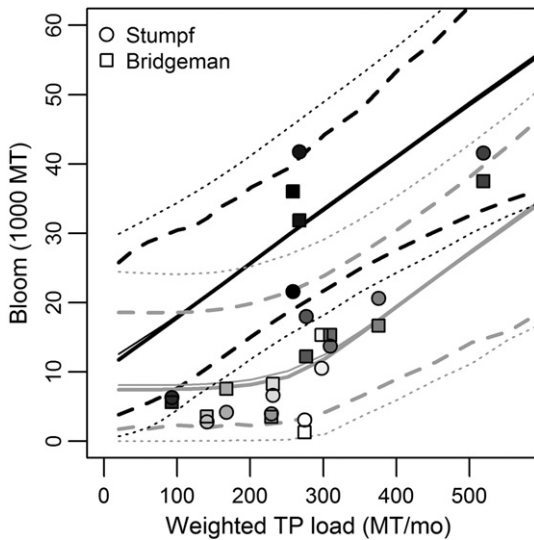

Fig.3. Load–response curves for cyanobacteria bloom size generated by the bioavailable P model. Bloom size is shown as a function of the overall weighted Maumee River TP load, which is the variable routinely measured by monitoring programs and directly addressed by the Nutrient Annex effort. The corresponding bioavailable P loads estimated by the model and used to generate the response curves are reported in ESM TableS1. The plot shows median predictions (thick lines), mean predictions (thin lines), 95% predictive intervals accounting for measurement error, model prediction error and parameter uncertainty (dotted lines), and 95% predictive intervals accounting for model prediction error and parameter uncertainty only (dashed lines). Gray lines: 2008 lake conditions; black lines: 2014 lake conditions. Bloom observations are shaded on a linear gradient from white (2002) to black (2014).
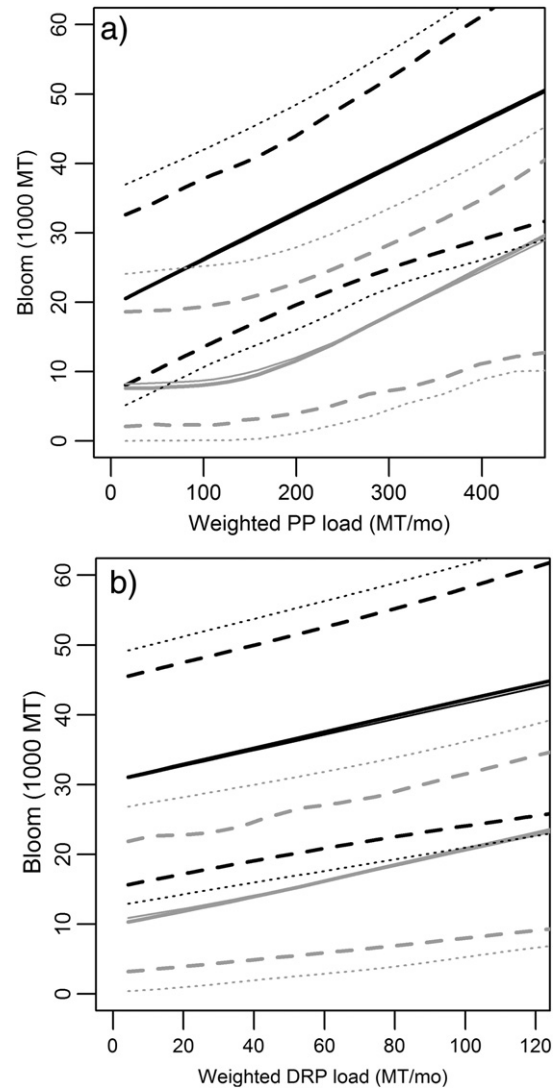

Fig.4. Load–response curves for cyanobacteria bloom size as a function of (a)weighted Maumee River PP load, while holding the DRP load to the 2008 value (79 MT/month) and (b)weighted Maumee River DRP load, while holding the bioavailable PP load to the estimated 2008 value (187 MT/month). The corresponding bioavailable P loads estimated by the model and used to generate the response curves are reported in ESM TablesS2–S3. The plots show median predictions (thick lines), mean predictions (thin lines), 95% predictive intervals accounting for measurement error, model prediction error and parameter uncertainty (dotted lines), and 95% predictive intervals accounting for model prediction error and parameter uncertainty only (dashed lines). Gray lines: 2008 lake conditions; black lines: 2014 lake conditions.

below 135 MT/month would be necessary (Fig.4a and TableS2). Finally, under the hypothetical scenario of a decrease in DRP load only, the model predicts that even if a highly unrealistic 95% reduction from the 2008 DRP load was achieved, bloom size would still be as high as 10,900 MT (95% predictive interval: 3500–21,700 MT, Fig.4b and ESM TableS3).

Under approximate 2014 conditions (black lines in Figs.3 and 4), the marked decrease in the load threshold estimated to trigger blooms above background level results in much larger mean predicted bloom size associated with the load reductions mentioned above (Figs.3 and 4 and ESM TablesS1, S2, and S3). For example, the model predicts that under 2014 conditions a TP load of 230 MT/month would still result in an average bloom size of 28,000 MT (95% predictive interval: 17,000–38,000 MT).

Discussion

Updated calibration data set

The decrease in predictive performance when calibrating to the revised and expanded sets of bloom observations suggests that the system may be undergoing complex non-linear dynamics that may no longer be best captured by the linear temporal trend included in the model. Specifically, the ratios of bloom size to spring Maumee TP and to DRP load, respectively, are markedly higher in 2013 (for both the Stumpf and the Bridgeman estimates) and in 2014 (for the Bridgeman estimate) than in previous years (ESM Fig.S1), supporting the hypothesis that the lake may be becoming more susceptible to cyanobacteria blooms over time, with smaller loads apparently triggering larger blooms in most recent years (Obenour etal., 2014). However, the limited number of years in the calibration data set prevents drawing definitive conclusions on the occurrence of a long-term trend in the system's vulnerability to HABs, and we cannot rule out the hypothesis that the larger deviations from model predictions observed in most recent years are at least partly the result of year-to-year variability not necessarily associated with a systematic trend.

The temporal trend estimated by the model can be viewed as a variable representing ecological processes that may be contributing to the recent HAB resurgence in western Lake Erie but are still not sufficiently well understood to be explicitly incorporated in the model. For example, it has been hypothesized that climate-driven changes in the frequency and timing of extreme spring rainfall events, followed by warm and calm summer conditions, might enhance bloom development (Michalak etal., 2013). Increased sediment P recycling and selective filter-feeding by invasive dreissenid mussels may also potentially favor cyanobacteria dominance (Arnott and Vanni, 1996; Conroy etal., 2005; Mellina etal., 1995; Vanderploeg etal., 2001). While zebra mussels have declined in the western basin since the 1990s, there is some evidence of an increase in the abundance of quagga mussels since the early 2000s (US EPA and Environment Canada, 2014). Although conclusive evidence on the basin-wide impact of mussels on bloom formation in recent years is still lacking for Lake Erie, a recent study of Lake Michigan illustrates how the density, distribution, and phytoplankton impacts of mussels have evolved over recent decades (Rowe etal., 2015). Finally, a change in the composition of the spring Maumee P load, and specifically an increase in the more readily bioavailable DRP load since the early 90s, have been suggested to play a role in the recent resurgence of HABs (Baker etal., 2014a). While the potential impacts of weather conditions and invasive species are not explicitly incorporated in the model, our results suggest that the increase in the DRP load alone may not be sufficient to explain the apparent increase in the lake's vulnerability to HABs. The DRP model explains a substantially smaller portion of the inter-annual variability in bloom size compared to the TP and bioavailable P models, confirming that the latter are better predictors of bloom intensity than DRP (Obenour etal., 2014; Stumpf etal., 2012). Furthermore, although the updated DRP model does not show an increase in the temporal trend parameter relative to Obenour etal. (2014), the parameter estimate remains significantly positive (ESM TableS4), indicating that replacing TP with DRP as the main bloom predictor does not eliminate the apparent positive trend in HAB susceptibility estimated by the model.

The decrease in the updated model performance is also partly associated with the marked discrepancy between the Stumpf and Bridgeman bloom estimates in 2013 and even more so in 2014 (Fig.1a), resulting in a considerable increase in the bloom measurement error component (σ_ϵ; Table 2 and ESM TableS4). The causes of these discrepancies are not completely understood, and they could be partly associated with method-specific spatiotemporal limitations that affect remote sensing vs. in situ bloom estimates (Ho and Michalak, 2015). For example, the in situ estimates are averages of bi-weekly samples collected at 6 stations, covering a limited area of approximately 340 km^2 in the vicinity of Maumee Bay (Bridgeman etal., 2013), while the remote sensing estimates are basin-wide, 10-day composites derived by summing the maximum observed (cloud-free) cyanobacteria biomass values across all image pixels (Stumpf etal., 2012). In addition, while in situ samples are taken over the whole water column, remote sensing estimates are typically representative of only the upper portion of the water column, thus potentially underestimating bloom size under well-mixed conditions (Wynne etal., 2010). The method used to calculate annual bloom size is also different, with the annual remote sensing estimates calculated as the maximum 30-day (i.e., 3 consecutive 10-day composites) moving average (Stumpf etal., 2012) and the annual in situ estimates derived by integrating bi-weekly bloom sizes over the whole summer (Bridgeman etal., 2013). The different calculation approaches may cause discrepancies between the two sets of annual bloom estimates if meteorological and hydrodynamic conditions result in the bloom persisting longer than usual in the vicinity of Maumee Bay, where the in situ sampling stations are located. However, no substantial differences in inter-annual variability emerge when comparing in situ annual bloom estimates obtained by integrating over the whole summer vs. calculating the maximum 30-day moving average ($R^2 = 97\%$).

In general, the differentiation of predictive and measurement error illustrates a key benefit of the hierarchical modeling approach (Cressie etal., 2009), which allows for representation of multiple sources of stochasticity and thus provides a more accurate quantification of overall predictive error and an improved understanding of the causes of increased uncertainty within the model. The updated calibration results indicate that uncertainty in bloom size characterization currently represents a substantial component of the overall uncertainty in HAB predictions. Studies aimed at filling this gap by developing methods to integrate multiple data sources and generate more accurate bloom estimates thus have the potential to reduce overall uncertainty in HAB size predictions.

Bioavailable P load as bloom predictor

The posterior mean for θ (0.63) is found to be slightly higher than the prior mean of 0.57. While the uncertainty in this posterior estimate is very large (Table2), the shift in the prior mean to a larger posterior value indicates the increase in likelihood that results from an enhanced contribution of PP, relative to DRP. This increase is also confirmed when using similarly vague priors for θ with smaller means (below 0.57) that also produce posterior means greater than 0.60 (not shown). In any case, the Bayesian approach allows for an explicit representation of the uncertainty associated with our prior knowledge of θ, and our (slightly) updated posterior knowledge of θ.

Although multiple studies have quantified the bioavailability of PP in the Maumee River (Table1), little observational information is available on the ultimate fate and availability of PP under in-lake conditions. Several in-lake processes might contribute to enhance the bioavailability of the PP load after it settles on the lake bottom, when compared to the bioavailability measured in the river. Most of the P load is typically delivered to the western basin in early spring (Stow etal., 2015), while *Microcystis* blooms typically initiate around mid-July and peak between August and September (Ho and Michalak, 2015; Wynne and Stumpf, 2015). During the lag period between load delivery and bloom growth, a portion of the organic PP pool could be regenerated as DRP through microbial mineralization and return to the water column through wind-induced mixing (Kleeberg and Dudel, 1997; Søndergaard etal., 1992). Furthermore, although the western basin does not undergo permanent seasonal stratification, intermittent stratification and subsequent transient bottom water hypoxic conditions have been repeatedly observed in the summer (Bridgeman etal., 2006; Britt, 1955; Britt etal., 1968; Carr etal., 1965; Loewen etal., 2007), potentially enhancing release of P from the sediment under reducing conditions (Behrendt etal., 1993; Holdren and Armstrong, 1980). Several experimental studies have also shown that invasive mussels can significantly enhance the rate at which PP is recycled into the water column as DRP, thereby decreasing

P turnover times and further increasing PP bioavailability to algae (Arnott and Vanni, 1996; Conroy etal., 2005; Mellina etal., 1995). Ecosystem-level studies quantifying the role of these in-lake processes in supplying P to fuel algal blooms could improve our understanding of the effective in-lake bioavailability of the PP load delivered to western Lake Erie. Such knowledge could be readily incorporated within a Bayesian modeling framework in the form of relatively narrower (more informative) prior distributions that could help reduce uncertainty in the estimates of weakly identifiable parameters.

Load–response scenarios

The Maumee spring TP load estimated by the model to result in a mean bloom size of 9600 MT under 2008 conditions (230 MT/month) is comparable to the values obtained by other cyanobacteria models included in the GLWQA Nutrient Annex multi-model effort (Stumpf etal., 2016-in this issue; Verhamme etal., 2016-in this issue). However, the width of the predictive intervals indicates that the uncertainty associated with model predictions needs to be taken into careful consideration when setting load targets, and it highlights the need to design appropriate adaptive management plans that can assess the lake's response to nutrient reductions and help decrease model predictive uncertainty as new knowledge is gained.

Results of the PP- vs. DRP-only reduction scenarios are also in agreement with the Western Lake Erie Ecosystem Model (WLEEM) simulations, with both models suggesting that even 100% removal of the Maumee DRP load alone would still result in unacceptable cyanobacteria blooms (Verhamme etal., 2016-in this issue). The cyanobacteria models adopted in the multi-model approach are based on somewhat different load periods, i.e., March–July for the models by Stumpf etal. (2016-in this issue) and Verhamme etal. (2016-in this issue) vs. approximately February–June for this model, as determined by Bayesian inference of the weighting parameter β_{lj}. Although the Maumee River P load shows some seasonality, with a large portion of the annual load delivered in early spring and relatively small loads in summer (July–September), there is substantial inter-annual variability in load seasonal timing (Stow etal., 2015). One notable example occurred in 2015, when intense precipitation in June led to substantially larger loads later in the season (June–July) than expected on average (http://www.heidelberg.edu/academiclife/distinctive/ncwqr/, accessed on 2 September 2015). As more observations become available, it may be possible to develop more sophisticated approaches to weighing monthly loads, providing further insights into the critical loading period.

Despite the good agreement with other models when considering 2008 conditions, the lake's apparent increasing susceptibility to large blooms estimated by the model (Obenour etal., 2014), further supported by the updated model calibration, led to an average predicted bloom size well above the 9600 MT threshold for a TP load of 230 MT/month under nearly current 2014 conditions (Fig.3). In fact, the model predicts that even at extremely low TP loads, bloom size could still be as high as 12,600 MT under current conditions (Fig.3). Although there is greater uncertainty in extrapolating bloom size values for small nutrient loads– for which extremely limited observations are available– it is reasonable to expect that even after substantial external load reductions, the internal P load accumulated over the years in the lake's sediments might continue to support high levels of primary production and delay the lake's response to watershed management actions (Bocaniov etal., 2016-in this issue; Chapra and Canale, 1991; Søndergaard etal., 2003; Welch and Cooke, 1995). In general, ecosystems have often been shown to undergo complex non-linear trajectories in response to changes in stressors due to shifts in internal feedbacks that may cause hysteretic behaviors (DeYoung etal., 2008; Scheffer and Carpenter, 2003; Scheffer etal., 2001) and/or concurrent changes in external drivers that influence ecosystem responses ("shifting baselines"; Carstensen etal., 2011; Duarte etal., 2009). The main implication of both the hysteresis and shifting baselines conceptual frameworks is that a system's response to a

decrease in the level of a stressor (e.g., nutrient loading) may deviate substantially from the system's behavior observed during the preceding phase of stress increase. Furthermore, in many aquatic systems, the level of nutrient reduction required to restore pre-eutrophication conditions was found to be substantially higher than the corresponding nutrient increase that led to the eutrophic state (Dokulil and Teubner, 2005; Duarte etal., 2009; Ibelings etal., 2007). The positive temporal trend estimated by the model appears consistent with this conceptual framework in indicating that the lake's response to nutrient loading may be changing over time, and a larger reduction in P load may be required to achieve a desired bloom threshold under current conditions compared to a decade ago (Figs.3 and 4).

The limitations of the available data should be taken into careful consideration when interpreting these results. The relatively small number of years in the calibration data set, coupled with the large year-to-year variability, currently limit our ability to adequately characterize the system's long-term behavior. Estimates of the temporal trend parameter are sensitive to individual years, as shown by the 38% increase in the parameter's estimate when adding two high-bloom years (2013 and 2014) to the calibration data set. It appears unlikely that this estimated rate of increase would continue in the long term, and the amount of data currently available is most likely not sufficient to provide a robust quantitative estimate of a potential long-term trend. While our results suggest that the system's response to stressors may be changing over time, a longer time series is needed to further test this hypothesis and, if verified, to elucidate the underlying mechanisms. As more years become available, more flexible temporal modeling approaches could be applied to better capture potential complex changes in the system's behavior that are not easily accommodated by a static temporal trend. For example, temporal shifts in the processes underlying system dynamics can be tracked through modeling approaches that allow parameters to evolve over time, such as dynamic linear models or weighted regression, where older information is discounted by giving earlier observations less weight as time progresses, so that at each time step parameter estimates are more strongly influenced by more recent years (Hirsch etal., 2010; Lamon etal., 1998, 1999).

A longer calibration data set would also allow for exploring additional predictors that are hypothesized to influence bloom size, such as hydro-meteorological factors or invasive mussel biomass. These factors may help decrease predictive uncertainty and explain potential changes in the system's behavior over time. Such efforts could significantly improve our ability to understand and control HABs, if coupled with an active adaptive management approach where evolving knowledge is incorporated into flexible predictive models that can capture complex ecosystem dynamics and update management strategies.

Acknowledgments

Appendix A. Supplementary Material

Supplementary data to this article can be found online at http://dx.doi.org/10.1016/j.jglr.2016.04.002.

References

Andersson, G., Gram, W., Stenson, J., Granéli, W., 1988. The influence of animals on phosphorus cycling in lake ecosystems. Hydrobiologia 170, 267–284.
Armstrong, D.E., Perry, J.J., Flatness, D.E., 1979. Availability of Pollutants Associated with Suspended or Settled River Sediments which Gain Access to the Great Lakes. US EPA GLNPO Report EPA-905/4–79-028, Chicago, IL.

Arnott, D.L., Vanni, M.J., 1996. Nitrogen and phosphorus recycling by the zebra mussel (*Dreissena polymorpha*) in the western basin of Lake Erie. Can. J. Fish. Aquat. Sci. 53, 646–659.

Baker, D.B., Confesor, R.B., Ewing, D.E., Johnson, L.T., Kramer, J.W., Merryfield, B.J., 2014a. Phosphorus loading to Lake Erie from the Maumee, Sandusky and Cuyahoga rivers: the importance of bioavailability. J. Great Lakes Res. 40, 502–517.

Baker, D.B., Ewing, D.E., Johnson, L.T., Kramer, J.W., Merryfield, B.J., Confesor, R.B., Richards, R.P., Roerdink, A.A., 2014b. Lagrangian analysis of the transport and processing of agricultural runoff in the lower Maumee River and Maumee Bay. J. Great Lakes Res. 40, 479–495.

Behrendt, H., Nixdorf, B., Pagenkopf, W.-G., 1993. Phenomenological description of polymixis and influence on oxygen budget and phosphorus release in Lake Müggelsee. Int. Rev. Gesamten Hydrobiol. Hydrogr. 78, 411–421.

Bocaniov, S., Leon, L., Rao, Y., Schwab, D., Scavia, D., 2016. Simulating the effect of nutrient reduction on hypoxia in central Lake Erie with a three-dimensional lake model. J. Great Lakes Res. 42, 1228–1240 (in this issue).

Boegman, L., Loewen, M.R., Hamblin, P.F., Culver, D.A., 2008. Vertical mixing and weak stratification over zebra mussel colonies in western Lake Erie. Limnol. Oceanogr. 53, 1093–1110.

Boström, B., Andersen, J.M., Fleischer, S., Jansson, M., 1988a. Exchange of phosphorus across the sediment–water interface. Hydrobiologia 170, 229–244.

Boström, B., Persson, G., Broberg, B., 1988b. Bioavailability of different phosphorus forms in freshwater systems. Hydrobiologia 170, 133–155.

Bridgeman, T.B., Schloesser, D.W., Krause, A.E., 2006. Recruitment of Hexagenia mayfly nymphs in western Lake Erie linked to environmental variability. Ecol. Appl. 16, 601–611.

Bridgeman, T.B., Chaffin, J.D., Kane, D.D., Conroy, J.D., Panek, S.E., Armenio, P.M., 2012. From river to lake: phosphorus partitioning and algal community compositional changes in western Lake Erie. J. Great Lakes Res. 38, 90–97.

Bridgeman, T.B., Chaffin, J.D., Filbrun, J.E., 2013. A novel method for tracking western Lake Erie Microcystis blooms, 2002–2011. J. Great Lakes Res. 39, 83–89.

Britt, N., 1955. Stratification in western Lake Erie in summer of 1953: effects on the Hexagenia (Ephemeroptera) population. Ecology 36, 239–244.

Britt, N., Skoch, E., Smith, K., 1968. Record low dissolved oxygen in the island area of Lake Erie. Ohio J. Sci. 68, 175–179.

Brittain, S.M., Wang, J., Babcock-Jackson, L., Carmichael, W.W., Rinehart, K.L., Culver, D.A., 2000. Isolation and characterization of microcystins, cyclic Heptapeptide Hepatotoxins from a Lake Erie strain of *Microcystis aeruginosa*. J. Great Lakes Res. 26, 241–249.

Carlton, J., 2008. The zebra mussel *Dreissena polymorpha* found in North America in 1986 and 1987. J. Great Lakes Res. 34, 770–773.

Carpenter, S.R., Cottingham, K.L., Schindler, D.E., 1992. Biotic feedbacks in lake phosphorus cycles. Trends Ecol. Evol. 7, 332–336.

Carr, J., Applegate, V., Keller, M., 1965. A recent occurrence of thermal stratification and low dissolved oxygen in western Lake Erie. Ohio J. Sci. 65, 319–327.

Carstensen, J., Sánchez-Camacho, M., Duarte, C.M., Krause-Jensen, D., Marbà, N., 2011. Connecting the dots: responses of coastal ecosystems to changing nutrient concentrations. Environ. Sci. Technol. 45, 9122–9132.

Cha, Y., Stow, C.A., 2015. Mining web-based data to assess public response to environmental events. Environ. Pollut. 198C, 97–99.

Chaffin, J.D., Bridgeman, T.B., Bade, D.L., 2013. Nitrogen constrains the growth of late summer cyanobacterial blooms in Lake Erie. Adv. Microbiol. 16–26.

Chapra, S.C., Canale, R.P., 1991. Long-term phenomenological model of phosphorus and oxygen for stratified lakes. Water Res. 25, 707–715.

Conroy, J.D., Edwards, W.J., Pontius, R.A., Kane, D.D., Zhang, H., Shea, J.F., Richey, J.N., Culver, D.A., 2005. Soluble nitrogen and phosphorus excretion of exotic freshwater mussels (Dreissena spp.): potential impacts for nutrient remineralisation in western Lake Erie. Freshw. Biol. 50, 1146–1162.

Cressie, N., Calder, C.A., Clark, J.S., Ver Hoef, J.M., Wikle, C.K., 2009. Accounting for uncertainty in ecological analysis: the strengths and limitations of hierarchical statistical modeling. Ecol. Appl. 19, 553–570.

DePinto, J.V., Young, T.C., Martin, S.C., 1981. Algal-available phosphorus in suspended sediments from lower Great Lakes tributaries. J. Great Lakes Res. 7, 311–325.

DePinto, J.V., Young, T.C., McIlroy, L.M., 1986. Impact of phosphorus control measures on water quality of the Great Lakes. Environ. Sci. Technol. 20, 752–759.

DeYoung, B., Barange, M., Beaugrand, G., Harris, R., Perry, R.I., Scheffer, M., Werner, F., 2008. Regime shifts in marine ecosystems: detection, prediction and management. Trends Ecol. Evol. 23, 402–409.

Dokulil, M.T., Teubner, K., 2005. Do phytoplankton communities correctly track trophic changes? An assessment using directly measured and palaeolimnological data. Freshw. Biol. 50, 1594–1604.

Duarte, C.M., Conley, D.J., Carstensen, J., Sánchez-Camacho, M., 2009. Return to Neverland: shifting baselines affect eutrophication restoration targets. Estuar. Coasts 32, 29–36.

GLWQA, 2012. The 2012 Great Lakes Water Quality Agreement—Annex 4. http://tinyurl.com/gt92hrh (Viewed 25 February 2016).

GLWQA, 2015. Recommended Phosphorus Loading Targets for Lake Erie—Annex 4 Objectives and Targets Task Team Final Report to the Nutrients Annex Subcommittee.

Guildford, S.J., Hecky, R.E., Smith, R.E.H., Taylor, W.D., Charlton, M.N., Barlow-Busch, L., North, R.L., 2005. Phytoplankton nutrient status in Lake Erie in 1997. J. Great Lakes Res. 31, 72–88.

Hirsch, R.M., Moyer, D.L., Archfield, S.A., 2010. Weighted regressions on time, discharge, and season (WRTDS), with an application to Chesapeake Bay river inputs. J. Am. Water Resour. Assoc. 46, 857–880. http://dx.doi.org/10.1111/j.1752-1688.2010.00482.x.

Ho, J.C., Michalak, A.M., 2015. Challenges in tracking harmful algal blooms: a synthesis of evidence from Lake Erie. J. Great Lakes Res. 41, 317–325.

Holdren, G.C., Armstrong, D.E., 1980. Factors affecting phosphorus release from intact lake sediment cores. Environ. Sci. Technol. 14, 79–87.

Ibelings, B.W., Portielje, R., Lammens, E.H.R.R., Noordhuis, R., Van Den Berg, M.S., Joosse, W., Meijer, M.L., 2007. Resilience of alternative stable states during the recovery ofshallow lakes from eutrophication: Lake Weluwe as a case study. Ecosystems 10, 4–16.

International Joint Commission, 1980. Biological Availability of Phosphorus (Windsor, CA).

Jetoo, S., Grover, V., Krantzberg, G., 2015. The Toledo drinking water advisory: suggested application of the water safety planning approach. Sustainability 7, 9787–9808.

Kleeberg, A., Dudel, G.E., 1997. Changes in extent of phosphorus release in a shallow lake (Lake Grosser Muggelsee; Germany, Berlin) due to climatic factors and load. Mar. Geol. 139, 61–75.

Lambert, R.S., 2012. Great Lakes Tributary Phosphorus Bioavailability Master's Thesis Michigan TechUniversityhttp://digitalcommons.mtu.edu/etds/250.

Lamon, E.C., Carpenter, S.R., Stow, C.a., 1998. Forecasting PCB concentrations in Lake Michigan salmonids: a dynamic linear model approach. Ecol. Appl. 8, 659–668. http://dx.doi.org/10.1890/1051-0761(1998)008[0659:FPCILM]2.0.CO;2.

Lamon, E.C.I., Carpenter, S.R., Stow, C.A., 1999. Rates of decrease of polychlorinated biphenyl concentrations in five species of Lake Michigan salmonids. Can. J. Fish. Aquat. Sci. 56, 53–59. http://dx.doi.org/10.1139/f98-147.

Lee, G., Jones, R., Rast, W., 1980. Availability of phosphorus to phytoplankton and its implications for phosphorus management strategies. In: Loehr, R., Martin, C., Rast, W. (Eds.), Phosphorus Management Strategies for Lakes. Ann Arbor Science, Ann Arbor, MI.

Loewen, M.R., Ackerman, J.D., Hamblin, P.F., 2007. Environmental implications of stratification and turbulent mixing in a shallow lake basin. Can. J. Fish. Aquat. Sci. 64, 43–57.

Logan, T.J., Oloya, T.O., Yaksich, S.M., 1979. Phosphate characteristics and bioavailability of suspended sediments from streams draining into Lake Erie. J. Great Lakes Res. 5, 112–123.

Lunn, D.J., Thomas, A., Best, N., Spiegelhalter, D., 2000. WinBUGS—a Bayesian modelling framework: concepts, structure, and extensibility. Stat. Comput. 10, 325–337.

Makarewicz, J., Lewis, T., Bertram, P., 1989. Phytoplankton and Zooplankton Composition, Abundance and Distribution and Trophic Interactions: Offshore Region of Lake Erie, Lake Huron, and Lake Michigan, 1985. Great Lakes National Program Office, US EPA (Chicago, IL).

Mellina, E., Rasmussen, J.B., Mills, E.L., 1995. Impact of zebra mussel (*Dreissena polymorpha*) on phosphorus cycling and chlorophyll in lakes. Can. J. Fish. Aquat. Sci. 2553–2573.

Michalak, A.M., Anderson, E.J., Beletsky, D., Boland, S., Bosch, N.S., Bridgeman, T.B., Chaffin, J.D., Cho, K., Confesor, R., Daloglu, I., Depinto, J.V., Evans, M.A., Fahnenstiel, G.L., He, L., Ho, J.C., Jenkins, L., Johengen, T.H., Kuo, K.C., Laporte, E., Liu, X., McWilliams, M.R., Moore, M.R., Posselt, D.J., Richards, R.P., Scavia, D., Steiner, A.L., Verhamme, E., Wright, D.M., Zagorski, M.A., 2013. Record-setting algal bloom in Lake Erie caused by agricultural and meteorological trends consistent with expected future conditions. Proc. Natl. Acad. Sci. U. S. A. 110, 6448–6452.

Obenour, D., Gronewold, A., Stow, C.A., Scavia, D., 2014. Using a Bayesian hierarchical model to improve Lake Erie cyanobacteria bloom forecasts. Water Resour. Res. 50, 7847–7860.

Perovich, G., Dortch, Q., Goodrich, J., Berger, P.S., Brooks, J., Evens, T.J., Gobler, C.J., Graham, J., Hyde, J., Karner, D., O'Shea, D.K., Paul, V., Paerl, H., Piehler, M., Rosen, B.H., Santelmann, M., Tester, P., Westrick, J., 2008. Causes, prevention, and mitigation. In: Hudnell, H.K. (Ed.), Cyanobacterial Harmful Algal Blooms—State of the Science and Research Needs. Springer, pp. 185–216.

R Core Team, 2015. R: ALanguage and Environment for Statistical Computing.

Reckhow, K., 1994. Importance of scientific uncertainty in decision-making. Environ. Manag. 18, 161–166.

Reckhow, K.H., Chapra, S.C., 1999. Modeling excessive nutrient loading in the environment. Environ. Pollut. 100, 197–207. http://dx.doi.org/10.1016/S0269-7491(99)00092-5.

Reinart, A., Kutser, T., 2006. Comparison of different satellite sensors in detecting cyanobacterial bloom events in the Baltic Sea. Remote Sens. Environ. 102, 74–85.

Rowe, M.D., Obenour, D.R., Nalepa, T.F., Vanderploeg, H.A., Yousef, F., Kerfoot, W.C., 2015. Mapping the spatial distribution of the biomass and filter-feeding effect of invasive dreissenid mussels on the winter–spring phytoplankton bloom in Lake Michigan. Freshw. Biol. 60, 2270–2285. http://dx.doi.org/10.1111/fwb.12653.

Scavia, D., Allan, J.D., Arend, K.K., Bartell, S., Beletsky, D., Bosch, N.S., Brandt, S.B., Briland, R.D., Daloğlu, I., DePinto, J.V., Dolan, D.M., Evans, M.A., Farmer, T.M., Goto, D., Han, H., Höök, T.O., Knight, R., Ludsin, S.A., Mason, D., Michalak, A.M., Richards, R.P., Roberts, J.J., Rucinski, D.K., Rutherford, E., Schwab, D.J., Sesterhenn, T.M., Zhang, H., Zhou, Y., 2014. Assessing and addressing the re-eutrophication of Lake Erie: central basin hypoxia. J. Great Lakes Res. 40, 226–246.

Scavia, D., DePinto, J.V., Bertani, I., 2016. A multi-model approach to evaluationg target phosphorus loads for Lake Erie. J. Great Lakes Res. 42, 1139–1150 (in this issue).

Schaeffer, B., Loftin, K., Stumpf, R., Werdell, P., 2015. Agencies collaborate, develop a cyanobacteria assessment network. EOS—Earth Space Sci. News 96. http://dx.doi.org/10.1029/2015EO038800.

Scheffer, M., Carpenter, S.R., 2003. Catastrophic regime shifts in ecosystems: linking theory to observation. Trends Ecol. Evol. 18, 648–656.

Scheffer, M., Carpenter, S., Foley, J.A., Folke, C., Walker, B., 2001. Catastrophic shifts in ecosystems. Nature 413, 591–596.

Søndergaard, M., Kristensen, P., Jeppesen, E., 1992. Phosphorus release from resuspended sediment in the shallow and wind-exposed Lake Arresø, Denmark. Hydrobiologia 228, 91–99.

Søndergaard, M., Jensen, J.P., Jeppesen, E., 2003. Role of sediment and internal loading of phosphorus in shallow lakes. Hydrobiologia 506-509, 135–145.

Srivastava, A., Singh, S., Ahn, C.Y., Oh, H.M., Asthana, R.K., 2013. Monitoring approaches for a toxic cyanobacterial bloom. Environ. Sci. Technol. 47, 8999–9013.

Steffen, M.M., Belisle, B.S., Watson, S.B., Boyer, G.L., Wilhelm, S.W., 2014. Status, causes and controls of cyanobacterial blooms in Lake Erie. J. Great Lakes Res. 40, 215–225.

Stow, C.A., Cha, Y., Johnson, L.T., Confesor, R., Richards, R.P., 2015. Long-term and seasonal trend decomposition of Maumee River nutrient inputs to western Lake Erie. Environ. Sci. Technol. 49, 3392–3400.

Stumpf, R.P., Wynne, T.T., Baker, D.B., Fahnenstiel, G.L., 2012. Interannual variability of cyanobacterial blooms in Lake Erie. PLoS One 7, e42444.

Stumpf, R., Johnson, L., Wynne, T., Baker, D., 2016. Forecasting annual cyanobacterial bloom biomass to inform management decisions in Lake Erie. J. Great Lakes Res. 42, 1174–1183 (in this issue).

Sturtz, S., Ligges, U., Gelman, A., 2005. R2WinBUGS: apackage for running WinBUGS from R. J. Stat. Softw. 12, 1–16.

US EPA, Environment Canada, 2014. State of the Great Lakes 2011. Indicators to Assess the Status and Trends of the Great Lakes Ecosystem.

Vanderploeg, H.A., Liebig, J.R., Carmichael, W.W., Agy, M.A., Johengen, T.H., Fahnenstiel, G.L., Nalepa, T.F., 2001. Zebra mussel (*Dreissena polymorpha*) selective filtration promoted toxic Microcystis blooms in Saginaw Bay (Lake Huron) and Lake Erie. Can. J. Fish. Aquat. Sci. 58, 1208–1221.

Verhamme, E., Redder, T., Schlea, D., Grush, J., Bratton, J., DePinto, J., 2016. Development of the western Lake Erie ecosystem model (WLEEM): application to connect phosphorus loads to cyanobacteria biomass. J. Great Lakes Res. 42, 1193–1205 (in this issue).

Welch, E.B., Cooke, G.D., 1995. Internal phosphorus loading in Shallow Lakes : importance and control. Lake Reserv. Manag. 11, 273–281.

Wynne, T.T., Stumpf, R.P., 2015. Spatial and temporal patterns in the seasonal distribution of toxic cyanobacteria in western Lake Erie from 2002 to 2014. Toxins (Basel) 7, 1649–1663.

Wynne, T.T., Stumpf, R.P., Tomlinson, M.C., Dyble, J., 2010. Characterizing a cyanobacterial bloom in western Lake Erie using satellite imagery and meteorological data. Limnol. Oceanogr. 55, 2025–2036.

Young, T.C., Depinto, J.V., Martin, S.C., Bonner, J.S., 1985. Algal-available particulate phosphorus in the Great Lakes Basin. J. Great Lakes Res. 11, 434–446.